



## Article

# The Fractionation of Corn Stalk Components by Hydrothermal Treatment Followed by Ultrasonic Ethanol Extraction

Nianze Zhang <sup>1,2</sup>, Chunyan Tian <sup>1,\*</sup> , Peng Fu <sup>1</sup>, Qiaoxia Yuan <sup>3</sup>, Yuchun Zhang <sup>1</sup>, Zhiyu Li <sup>1</sup>  and Weiming Yi <sup>2</sup>

<sup>1</sup> School of Agricultural Engineering and Food Science, Shandong University of Technology, Zibo 255000, China; 19403010075@stumail.sdut.edu.cn (N.Z.); fupeng@sdut.edu.cn (P.F.); zhangyc@sdut.edu.cn (Y.Z.); lizhiyu@sdut.edu.cn (Z.L.)

<sup>2</sup> Shandong Research Center of Engineering and Technology for Clean Energy, Zibo 255000, China; yiweiming@sdut.edu.cn

<sup>3</sup> College of Engineering, Huazhong Agricultural University, Wuhan 430070, China; qxyuan@mail.hzau.edu.cn

\* Correspondence: tiancy@sdut.edu.cn

**Abstract:** The fractionation of components of lignocellulosic biomass is important to be able to take advantage of biomass resources. The hydrothermal–ethanol method has significant advantages for fraction separation. The first step of hydrothermal treatment can separate hemicellulose efficiently, but hydrothermal treatment affects the efficiency of ethanol treatment to delignify lignin. In this study, the efficiency of lignin removal was improved by an ultrasonic-assisted second-step ethanol treatment. The effects of ultrasonic time, ultrasonic temperature, and ultrasonic power on the ultrasonic ethanol treatment of hydrothermal straw were investigated. The separated lignin was characterized by solid product composition analysis, FT-IR, and XRD. The hydrolysate was characterized by GC-MS to investigate the advantage on the products obtained by ethanol treatment. The results showed that an appropriate sonication time (15 min) could improve the delignification efficiency. A proper sonication temperature (180 °C) can improve the lignin removal efficiency with a better retention of cellulose. However, a high sonication power 70% (840 W) favored the retention of cellulose and lignin removal.

**Keywords:** ultrasonic; components fractionation; lignocellulose; ethanol treatment



**Citation:** Zhang, N.; Tian, C.; Fu, P.; Yuan, Q.; Zhang, Y.; Li, Z.; Yi, W. The Fractionation of Corn Stalk Components by Hydrothermal Treatment Followed by Ultrasonic Ethanol Extraction. *Energies* **2022**, *15*, 2616. <https://doi.org/10.3390/en15072616>

Academic Editors: Andrea Di Carlo and Elisa Savuto

Received: 15 March 2022

Accepted: 30 March 2022

Published: 3 April 2022

**Publisher's Note:** MDPI stays neutral with regard to jurisdictional claims in published maps and institutional affiliations.



**Copyright:** © 2022 by the authors. Licensee MDPI, Basel, Switzerland. This article is an open access article distributed under the terms and conditions of the Creative Commons Attribution (CC BY) license (<https://creativecommons.org/licenses/by/4.0/>).

## 1. Introduction

Biomass use is becoming increasingly important with the growing concern related to the development of sustainable energy sources [1]. There are many types of biomass resource available, such as lignocellulosic biomass (LCB) consisting of cellulose, hemicellulose and lignin, food waste, and manure [2]. Corn stalk, a typical representative of lignocellulose, is often burned in an open environment, causing a great environmental pollution problem, and the wasting of this resource at the same time. Corn stalk is abundant in storage, accounting for about 32.46% of the total straw, and has great potential for application. Corn stalk can be converted to obtain biofuels or high value-added chemicals [3]. In recent years, the efficient conversion and utilization of corn stalk has become a research hotspot [4,5].

The complex structural features of LCB protect its carbohydrates from microbial or enzymatic degradation [6,7]. The recalcitrance of LCB stems mainly from the structural properties of the plant cell wall; it is a network mechanism formed by the cross-linking of xylans and lignin, so when utilizing LCB, it is first necessary to separate the composite tissue into each component to further enhance the value [8].

The pulp industry has developed several separation techniques that use strong acid or base reagents to separate lignin from the lignocellulosic biomass by decomposing and dissolving the lignin into the liquid [9]. However, this method of treatment only targets the utilization of cellulose and does not consider lignin and hemicellulose as resources, generating great waste. During the recovery of lignin, lignin condensation is produced,

resulting in a limitation of recovered lignin, so this treatment is not applicable to the recovery of lignin.

Organic solvent treatment is a future component fractionation green technology [10]. The organic solvent treatment method allows lignin and hemicellulose to be dissolved in an aqueous organic solvent. In contrast to acid or alkali treatment, an organic solvent treatment prevents changes in the lignin structure due to its mild conditions. When treating lignocellulosic biomass by organic solvents, the lignin can be dissolved into the organic solvent solution and the cellulose is retained in the solid. Due to the aromatic nature of the lignin fragments, lignin is freely dissolved in organic solvents [11]. Organic solvent pretreatments usually include organic acids or alcohols, such as acetic acid, acetone and ethanol. Most organic solvents have low boiling points and can be easily separated. The usual conditions for organic solvent pretreatment are 1–3 h at 150 °C to obtain 60–90% lignin removal. Glucose yields in organic solvent pretreatment biomass saccharification range from 46% to 99% [12].

Already widely used in other areas, ultrasounds can be used to enhance the separation efficiency of components in lignocellulosic biomass. Ultrasound is a green technology that has the advantage of reducing energy consumption and causes less pollution [13]. Ultrasounds can break the complex structure of lignocellulose and remove hemicellulose and lignin, allowing various chemical reagents to better bind to the cellulose and facilitate the reaction. As a result, ultrasonic technology has been widely valued and developed for biomass pretreatment [14,15]. According to reports, the ultrasonic treatment of biomass increases the crystallinity of biomass and accomplishes the separation of the three major components. Cellulose is present in solid form and lignin and hemicellulose are dissolved into the solvent. However, the application of ultrasounds in LCB is still in its infancy. Nevertheless, there are relatively few studies on adding ultrasonic assistance to the process of treating biomass with organic solvents, so the application of ultrasound should be expanded.

The hydrothermal–ethanol method, which combines an organic solvent treatment and hydrothermal treatment, has gained importance [16,17]. The efficiency of the hydrothermal–ethanol method for the separation of lignin is lower than that of the organic solvent treatment. The biomass is hydrothermally treated and the lignin is removed from the cell walls, but with cooling, microspheres are formed that reattach to the cellulose surface. The hydrothermally treated biomass is then subjected to ethanol treatment, which causes this portion of the lignin microspheres to re-polymerize and form a lignin coating to attach to the cellulose surface, thus leading to a significant impact on the efficiency of lignin removal. Therefore, the focus of the study shifted to how to improve the low efficiency of lignin removal in the hydrothermal–ethanol method [18].

The characteristic point of this study is the combination of hydrothermal treatment, ethanol treatment, and ultrasonic treatment, which combines the advantages of the three treatments to achieve a stepwise separation of the three major components of LCB. By hydrothermal treatment, the hemicellulose component of corn stalk was removed. The lignin component was removed from the corn stalk by ultrasound-assisted ethanol. Finally, cellulose-rich solids were obtained. The problem of the low efficiency of lignin removal by the hydrothermal–ethanol method was solved with the aid of an ultrasound.

In this study, the goal was set to explore the problem and to improve the efficiency of lignin removal by the hydrothermal–ethanol method. This study used corn stalks as a feed-stock. By studying the ultrasonic time, ultrasonic temperature, and ultrasonic power, the aim was to obtain an efficient and clean fraction separation technique. With the aid of an ultrasound, the problem of the low efficiency of lignin removal by the hydrothermal–ethanol method can be effectively solved, which is beneficial for the separation and utilization of cellulose, lignin, and hemicellulose.

## 2. Materials and Methods

### 2.1. Raw Materials and Analytical Methods

The corn stalk was obtained from Jiangsu province, China, crushed through a grinder, and then the obtained corn stalk powder was sieved through an environmentally friendly vibrating sieve machine (SDNS 300t, Hubei, China) to obtain 40–60 mesh corn stalk. The obtained corn stalk was subjected to hydrothermal treatment at 180 °C and solid–liquid separated in an autoclave (Parr 4575a, Moline, IL, USA) with water as a solvent, and the resulting solid product was dried in an electric thermostatic drying oven (WGL-858, Hebei, China) at 105 °C, which is the hydrothermal straw (HT) required for this experiment.

### 2.2. Ultrasonic-Assisted Ethanol Treatment of Hydrothermal Straw

The separation of the components was completed according to the hydrothermal–ethanol method [17,18]. The problem of low lignin removal efficiency was solved by attaching ultrasonic assistance to the second ethanol treatment step. Fixed factors: solids content 5 ω%, ethanol concentration 50 φ%, material as HT, pulse 2 s/8 s. The effects of ultrasonic time, ultrasonic temperature, and ultrasonic power on lignin removal efficiency were investigated in a single-factor test. The ultrasonic generator was selected from an ultrasonic processor (Jy98-222DN, Beijing, China) with 1200 W and φ20 variable amplitude rod, and the ultrasonic power was output in a percentage. The ultrasonic temperature was set at 140 °C, ultrasonic power at 40%, and the experiment was set at the ultrasonic times of 0, 15, 30, 45, 60 min. The ultrasonic time was set to 30 min, ultrasonic power was set to 40%, and the experiment was set with ultrasonic temperatures of 100, 120, 140, 160, 180 °C. The sonication time was set to 30 min, sonication temperature was set to 140 °C, and the experiment was set with sonication powers of 10, 25, 40, 55, 70%. After the treatment was completed, the mixture was filtered through a Brinell funnel, the solid was dried in a blast drying oven at 105 °C to a constant weight, and the liquid was centrifuged to obtain ethanolic lignin. Figure 1 shows the overview of the hydrothermal–ethanol treatment.

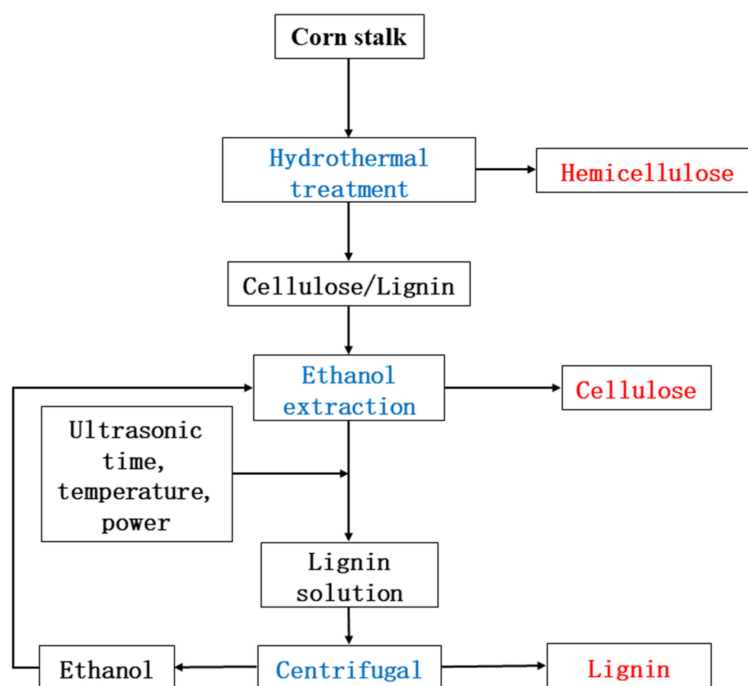


**Figure 1.** The overview of hydrothermal—ultrasonic ethanol treatment.

### 2.3. Analysis and Calculation Methods

#### 2.3.1. Hydrolysate Composition Analysis

The compositional changes in the liquid phase products were identified using a gas chromatography–mass spectrometry (GC–MS) analyzer (Agilent 5973-6080, Santa Clara, CA, USA). The column used for the test samples was DB-1701. The aqueous phase was extracted with Dichloromethane, filtered with a 0.22 µm filter membrane, and determined on the machine. The initial temperature was 40 °C, and the temperature was increased at 5 °C/min to 240 °C for 5 min; the shunt ratio was 30:1; and the solvent was delayed for 2 min [19]. The NIST17.L mass spectrometry library was used to compare with the compounds and to select the identified components.

#### 2.3.2. Fourier Transform Infrared Spectrometry (FT-IR) Analysis

A Fourier infrared spectrometer (Thermo Nicolet 5700, Thermo Electron, Waltham, MA, USA) was used to qualitatively analyze the functional groups and the chemical bonds of the solid products to determine the changes in the components during the separation process [20,21]. The wavelength range was 400–4000 cm<sup>−1</sup> with a resolution better than 0.09 cm<sup>−1</sup> and a wavenumber accuracy of 0.01 cm<sup>−1</sup>.

#### 2.3.3. Content of Cellulose, Lignin, and Hemicellulose Fractions in Solid Products

The content of cellulose, lignin, and hemicellulose fractions in solid products based on the Van Soest principle was measured using a cellulose tester (ANKOPM A220i, Macedon, NY, USA) [22–24]. The sample was boiled and treated by neutral detergent, and the undissolved residue was neutral detergent fiber, which is mainly cell wall components, including hemicellulose, cellulose, acid insoluble lignin and silicate. The sample was treated with acid detergent, and the remaining residue was acid detergent fiber, which included cellulose, acid insoluble lignin and silicate, and the difference between neutral detergent fiber and acid detergent fiber was the hemicellulose content. The residue of acid detergent fiber after 72% sulfuric acid treatment was acid insoluble lignin and silicate, and the cellulose content of the sample was obtained by subtracting the residue after 72% sulfuric acid treatment from the acid detergent fiber value. The residue after 72% sulfuric acid treatment was dried and then ashed, and the part that escaped during the ashing process was the acid-washed lignin content.

#### 2.3.4. X-ray Diffractometry (XRD) Analysis

The fiber crystal structure in the obtained solid products was characterized by an X-ray diffractometer (D8-02, Karlsruhe, Germany) [25,26]. The dried sample was put into the test piece, the glass press was used to flatten the test piece to keep the surface flat, then the test piece was put into the sample holder. The test conditions: Diffraction angle 2 min scans were performed in the range 5–60°, angular resolution: FWHM(Full Width at Half Maxima) ≤ ±0.1; angular reproducibility: ±0.0001°.

#### 2.3.5. Calculation Methods of Evaluation Indicators

Calculation of yields of solid yield, cellulose retention rate, and lignin extraction rate [16]. The calculation method in the text is as follows:

$$\text{solid yield (d\%)} = \frac{\text{Solid mass}}{\text{Stalk mass}} \times 100\% \quad (1)$$

$$\text{Cellulose retention rate (d\%)} = \frac{\text{Solid cellulose mass}}{\text{Stalk cellulose mass}} \times 100\% \quad (2)$$

$$\text{Lignin extraction rate (d\%)} = 1 - \frac{\text{solid lignin mass}}{\text{Stalk lignin mass}} \times 100\% \quad (3)$$

Stalk mass is the mass of reactants, solid mass is the mass of the solid product obtained by the reaction, the solid cellulose mass is the mass of cellulose in the solid product, the

stalk cellulose mass is the mass of cellulose in the stalk, the solid lignin mass is the mass of lignin in the solid product, and the stalk lignin mass is the mass of lignin in the stalk.

### 3. Results and Discussion

#### 3.1. Characteristics of Raw Materials

Table 1 shows the characteristics of the corn stalk and hydrothermal stalk. From the table, the contents of the three components of the hydrothermal stalk and corn stalk can be seen.

**Table 1.** Characteristics of corn stalk and hydrothermal stalk.

Components	Corn Stalk	Hydrothermal Stalk
Chemical composition (daf%)		
Hemicellulose	31.31 ± 0.69	8.22 ± 0.14
Cellulose	40.13 ± 0.40	57.06 ± 1.11
Lignin	9.74 ± 0.87	23.15 ± 0.56

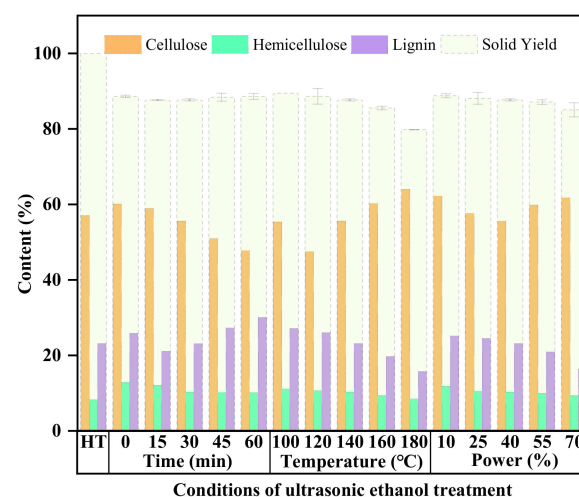
The number after ± denotes Standard Deviation.

The hydrothermal–ethanol method is a good method for the separation of ligno-cellulosic biomass fractions. The hydrothermal treatment of corn stalk released 90% of hemicellulose and had a high hemicellulose separation efficiency.

#### 3.2. Effect of Different Conditions of Ultrasonic Ethanol Treatment on Solid Products

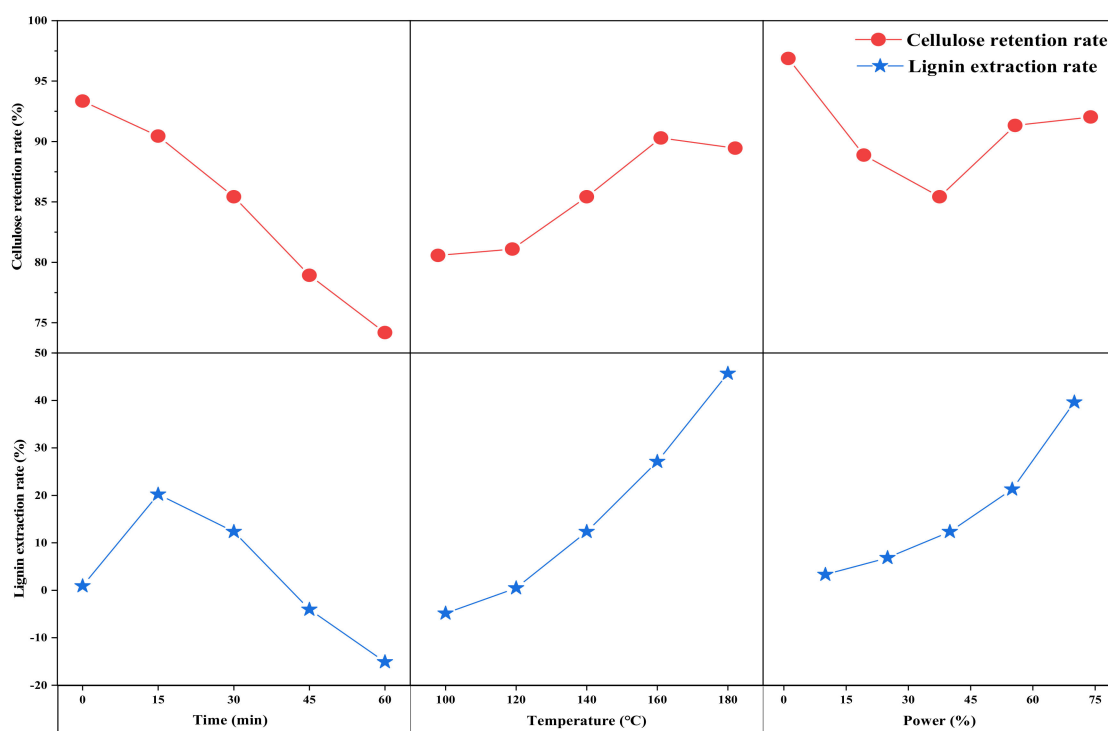
##### 3.2.1. Effect of Different Times of Ultrasonic Ethanol Treatment on a Solid Product

Figure 2 shows the effect of the time factor on the three main components and yields of the solid products. Compared with the control sample, the ultrasonic ethanol treatment had a significant effect on the yield of the solid product, and the mass loss was more than 10%, which may have been partially caused by the loss of various components of the corn stalk. With the increase in the ultrasonic time, the change in the mass decreased and then increased, and reached an inflection point at 15 min of ultrasonic time. Before 15 min, the mass kept reducing with the increase in time, and the lowest point reached 87.65%. The mass kept increasing again when the time exceeded 15 min. From the experimental results, it is clear that the hydrothermal straw was treated with ethanol by ultrasonication, and many substances were precipitated from the solid, which may partly be the presence of cellulose, lignin, hemicellulose, and soluble substances present in the straw, so the composition of the solid product needs to be analyzed to elucidate the effect of ultrasonication time on the dissolution of hydrothermal stalk [2,20].



**Figure 2.** Effect of different ultrasonic ethanol treatments on solid product yields and fractions.

Figure 3 shows the effect of the time factor on the cellulose retention and lignin removal of the solid products. Cellulose retention and lignin removal are important indicators used to judge the effectiveness of ultrasonic ethanol treatment [27,28]. In the process of exploring the ultrasonic time on ethanol treatment, the retention of cellulose decreased continuously with the increase in time and showed a linear relationship with R2 reaching 0.9831 and the equation  $y = -4.9836x + 99.414$ , the retention of cellulose decreased from 93.34% at 0 min to 74.18% at 60 min. Moreover, the lignin removal efficiency was the opposite of the mass change, which rose and then decreased, the inflection point appeared at 15 min, the lignin removal efficiency was 20.20%, and with the increase in time, the lignin removal efficiency gradually decreased. At 60 min, it reached  $-15.08\%$ , indicating that with the increase in time, the condensation of the removed lignin occurred, resulting in more lignin content and more lignin in the solid product of the attached lignin.



**Figure 3.** Lignin removal and cellulose retention of solid products.

The ultrasonic treatment destroys wax-containing and silicon-containing components deposited on the lignocellulosic surface [29,30] which is the main reason for the change in mass. Hydrothermal straw was treated with ultrasound-assisted ethanol, which allows this part of the fraction to be dissolved, as seen in the 0 min group, which was effectively removed under the action of ultrasound [15].

The effect on the loss of mass as the time increased, as can be seen from Figures 1 and 2, was due to mass changes in cellulose and lignin. When ultrasound acts on cellulose, the penetration of heat into the fiber structure is enhanced due to the sonar effect generated by ultrasound, and the high temperature and pressure provide conditions for the unbinding of the hydrogen bonds of cellulose molecules [31]. These effects cause damage to the cellulose surface and interior, and the morphological structure is disrupted so that part of the cellulose is hydrolyzed during the treatment. The presence of ultrasound can also destroy the lignin microspheres deposited on the surface of lignocellulose [16]. At the same time, it can also act internally to break the joints between lignin and cellulose, allowing the lignin to break away from the entire structure and dissolve into the organic solvent ethanol [32,33]. As the treatment time increases, the ultrasonic treatment causes condensation and the degradation of lignin, which dissolves from hydrothermal straw into the solution while



releasing low molecular weight phenols that clear the free radicals released during the instantaneous collapse. This leads to the polymerization of lignin and deposition on the biomass surface, resulting in an increase in lignin mass and a negative lignin removal efficiency [34–36].

### 3.2.2. Effect of Ultrasonic Ethanol Treatment at Different Temperatures on a Solid Product

Figure 2 shows the effect of the temperature factor on the three main components and yields of the solid products. As the temperature increased, the yield of the solid product obtained gradually decreased. The analysis of the first three points and the linear fit revealed that  $R^2$  was equal to 0.9989, obtaining the function  $y = -0.89x + 90.387$ , which indicates that at low temperatures, the mass loss increases linearly with temperature, and when the temperature is higher than 140 °C, the rate of mass loss increases and more material undergoes hydrolysis and is removed from the solid, which may be part of hemicellulose, lignin, and part of cellulose [37,38].

Figure 3 shows the effect of the temperature factor on the cellulose retention and lignin removal of the solid products. The changes of each component in the hydrothermal straw with temperature changes can be better analyzed [39]. The cellulose retention showed rose and then fell, the inflection point was at 160 °C, the retention rate reached the highest at 90.29%, and the lignin removal rate was a linear rising trend. When the point of 100 °C was excluded, a linear fit to the remaining temperature points could be obtained as a linear function  $y = 15.032x - 6.176$ .  $R^2$  was equal to 0.9901, which is consistent with the linear law, indicating that the lignin removal rate was linearly and positively correlated with the temperature. This indicates that after hydrothermal treatment, hemicellulose was removed from the straw and the three components of lignocellulose caused the dense structure to be destroyed. Cellulose can only be hydrolyzed at low temperatures. With the increase in temperature, the lignin removal rate increased, the detached lignin in solution was constantly polymerized, attached, and removed, and the increase in lignin molecules and the increase in the active degree of cellulose played a good protective role. In the investigation of the effect of temperature on the hydrothermal straw fraction, the loss of mass is directly related to the rate of lignin removal [40,41].

### 3.2.3. Effect of the Different Powers of Ultrasonic Ethanol Treatment on a Solid Product

Figure 2 shows the effect of the ultrasonic power factor on the three main components and yields of the solid products. As the ultrasound power increases, the quality of the solid product obtained after treatment constantly decreases. The increase in ultrasonic power and the cavitation bubbles lead to the fragmentation of the cell wall and an increase in the permeability of the solvent, which leads to a continuous loss of mass quality [42].

Figure 3 shows the effect of the ultrasonic power factor on the cellulose retention and lignin removal rate of the solid products. As can be seen in Figure 2, the lignin removal rate increased with the increase in ultrasonic power, and the efficiency of lignin removal rate increased, indicating that the ultrasonic power had a significant effect on the release of lignin. The cellulose retention rate decreased and then increased with the increase in power, and the cellulose retention rate reached the lowest value at 40% power. This is mainly due to the cavitation effect of ultrasound, which leads to the breaking of aryl ether bonds in lignin, and the breaking of hydrogen bonds between lignin and cellulose [43,44]. This promotes the release and dissolution of more lignin into the organic solvent. Thus, an increase in ultrasonic power can enhance the cavitation effect, which leads to an increase in the lignin removal efficiency [14,45].

### 3.3. Effect of Different Conditions of Ultrasonic Ethanol Treatment on the Properties of Solid Products

The FT-IR spectra of the solid products obtained with different sonication factors are shown in Figures 4–6. Their FT-IR spectra are very similar and agree with reports found in the literature [46–49]. The infrared absorption wave numbers of cellulose OH and C–O are 3200–3400 and  $\sim 1050\text{ cm}^{-1}$ , and those of hemicellulose C=O (from ketone and carboxyl

groups) and C-C (from sugar skeleton) are  $1715 \sim 1765$  and  $615 \text{ cm}^{-1}$ , respectively; lignin is rich in O-CH<sub>3</sub> (from methoxy), C-O-C (from the aromatic-alcohol ester bond), C=C (from the aromatic ring) and C-OH (from phenolic hydroxyl group), whose wave numbers are located at  $1430 \sim 1270$ ,  $1270$ ,  $1450$  and  $1613$ ,  $1215 \text{ cm}^{-1}$ .

For the solid products treated with different ultrasonic factors of ethanol, the solid products were compared according to the characteristic peaks of infrared spectra. It was found that the characteristic peaks of hemicellulose were undetectable, indicating the removal effect of hemicellulose in the treatment process. In addition, comparing the characteristic peaks of cellulose and lignin, the signals of these two components were obvious, which, combined with the retention rate of cellulose and the removal rate of lignin, proved that cellulose and lignin were still present in the solid products obtained after the ethanol treatment with ultrasound.

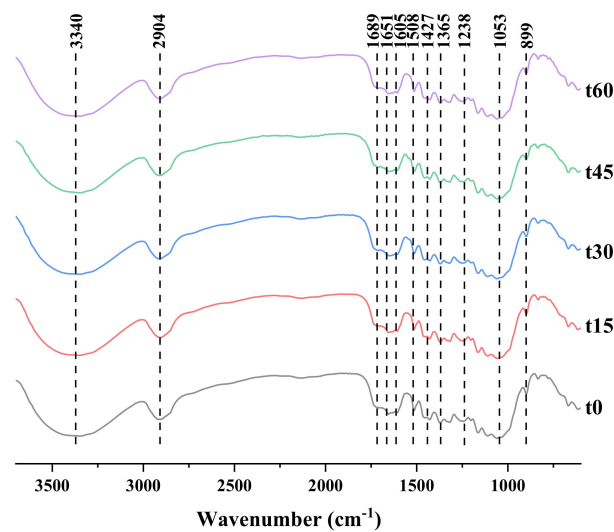


**Figure 4.** Infrared spectra of corn stalk treated with different ultrasound times.

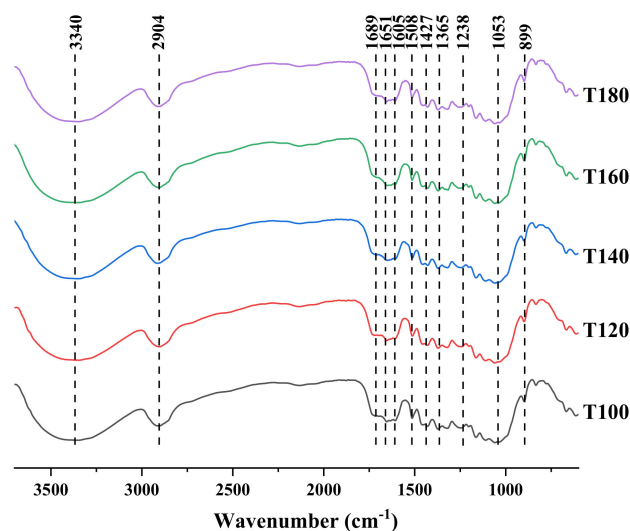


**Figure 5.** Infrared spectra of corn stalk treated with different ultrasound temperatures.



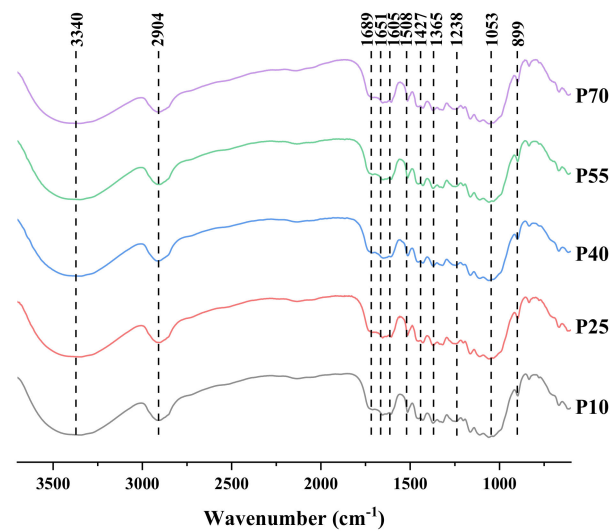


**Figure 6.** Infrared spectra of corn stalk treated with different ultrasonic power.

The solid products obtained were analyzed by XRD and the results of the calculated cellulose crystallinity are listed in Table 2. From Table 2, we can see that after sonication, the crystallinity of type I and type II cellulose changed. With the increase in sonication time, type I cellulose decreased, then increased, and then decreased, and the inflection points existed at 15 min and 45 min, with a maximum value of 40.43% and a minimum value of 34.06%. Type II cellulose rose and then fell, and the inflection point existed at 45 min, reaching a maximum value of 44.06%. With the increase in the ultrasonic temperature, type I cellulose decreased and then increased, the inflection point appeared at 120 °C, reached a minimum value of 29.49%, and then with the increase in temperature until 180 °C, reached a maximum value of 40.38%. Type II cellulose decreased and then increased, with the inflection point appearing at 100 °C, reaching a minimum value of 30.70%, and then reaching a maximum value of 42.67% with the increase in temperature up to 180 °C. With the increase in ultrasonic power, type I cellulose rose and then fell, and then rose and then decreased, reaching an inflection point at 25%, reaching a maximum value of 37.28% at 55% power, and a minimum value of 28.92% at 70% power. Type II cellulose showed the same trend as type I cellulose, reaching a maximum value of 39.93% at 55% power and a minimum value of 35.03% at 70% power.

**Table 2.** Crystallinity of solid products.

		CrI-I	CrI-II
Time (min)	HT	35.54	37.64
	0	34.47	38.22
	15	34.06	39.05
	30	36.48	39.79
	45	40.43	44.06
	60	39.93	39.56
Temperature (°C)	100	30.01	30.70
	120	29.49	32.24
	140	36.48	39.79
	160	38.05	41.16
	180	40.39	42.67
Power (%)	10	35.54	38.62
	25	33.44	37.74
	40	36.48	39.79
	55	37.28	39.94
	70	28.92	35.03

With the enhancement of ultrasonic conditions, type I cellulose transforms to type II cellulose, and cellulose crystallinity increases, which is mainly due to the removal of lignin and hemicellulose from lignocellulose and the hydrolysis of the amorphous zone. Ultrasonic waves promote the removal of lignin and hemicellulose, which makes the cellulose content increase relatively, thus leading to the increase in crystallinity [49,50]. When it reaches 45 min, the crystallinity starts to decrease, which is mainly due to the destruction of cellulose crystals caused by the ultrasonic waves on the hydrogen bonds between cellulose molecules, in addition to the re-polymerization of lignin, which leads to the reduction in cellulose content, both of which lead to the decrease in crystallinity [51].

### 3.4. Effect of Different Conditions of Ultrasonic Ethanol Treatment on the Characteristics of Liquid Products

The composition of the liquid products obtained by different ultrasonic ethanol treatments was analyzed, and the specific composition distribution is listed in Table 3. For the liquid products obtained by ultrasonic ethanol treatment, excluding the two added solvents of water and ethanol, the composition of other components was the same. Ethyl formate was the main product, which is mainly the hemicellulose and cellulose hydrolysis of five-carbon sugar and six-carbon sugar. After the reaction, they were first converted to furfural, then furfural in the ethanol  $H^+$  ionized in the process of treatment into furfuryl alcohol, and hydrolysis occurred under the catalytic effect of  $H^+$  to obtain ethyl formate [52,53].

**Table 3.** GC-MS composition analysis of ultrasonic ethanol-treated liquid products.

RT (min)		3.85	4.74	5.77	7.37	27.62
		Formic acid, ethenyl ester $C_3H_4O_2$	Ethyl formate $C_3H_6O_2$	Ethyl Acetate $C_4H_8O_2$	1,1-diethoxy- Ethane, $C_6H_{14}O_2$	2-methyl- Benzaldehyde, $C_8H_8O$
Time (min)	0	4.65	87.58	1.14	3.16	3.48
	15	6.38	88.62	1.23	3.77	-
	30	5.90	90.69	-	3.41	-
	45	4.72	85.47	1.28	3.69	4.84
	60	5.50	88.33	0.92	4.11	1.13
Temperature (°C)	100	3.69	92.56	0.93	2.82	-
	120	3.54	93.28	1.11	2.07	-
	140	5.90	90.69	-	3.41	-
	160	4.97	85.58	1.82	5.34	2.29
	180	20.96	46.26	3.66	19.18	9.95
Power (%)	10	19.28	58.37	12.19	10.16	-
	25	36.00	30.77	20.37	12.87	-
	40	5.90	90.69	-	3.41	-
	55	8.87	74.86	8.50	7.76	-
	70	30.25	22.17	15.45	7.78	24.35

### 3.5. Characterization of Ethanol Lignin

Figures 7–9 show the fingerprint regions of the lignin FT-IR spectra. According to the literature, the plots were analyzed to obtain the types of various characteristic peaks [54–58]. The peaks at 1601, 1509, and 1423  $cm^{-1}$  belong to the benzene ring vibration of the benzene propane skeleton; the absorption peak at 1367  $cm^{-1}$  demonstrates the presence of S-type and condensed cross-linked G-type lignin structural units; 1238  $cm^{-1}$  is characteristic of G-type lignin structural units; 1329  $cm^{-1}$  is characteristic of S-type lignin structural units; the 1121  $cm^{-1}$  peak indicates the C-H bond deformation vibration in S-type lignin; and 1033  $cm^{-1}$  indicates C-H bond deformation vibration in G-type lignin. The 832  $cm^{-1}$  peak is the out-of-plane bending in  $C_{2,6}$  of the S-type lignin unit. The C=O stretching vibration was at 1720  $cm^{-1}$ , the conjugated aryl carbonyl group stretching at was at 1657  $cm^{-1}$ , the C-H deformation and methoxy bending was at 1455  $cm^{-1}$ , and the methyl acetate

C-H stretching was at  $1367\text{ cm}^{-1}$ . The FT-IR spectra were very similar, and the relative intensities of the characteristic peaks were almost unchanged, indicating similar changes in the chemical structure of the lignin obtained by the ultrasonic ethanol treatment.

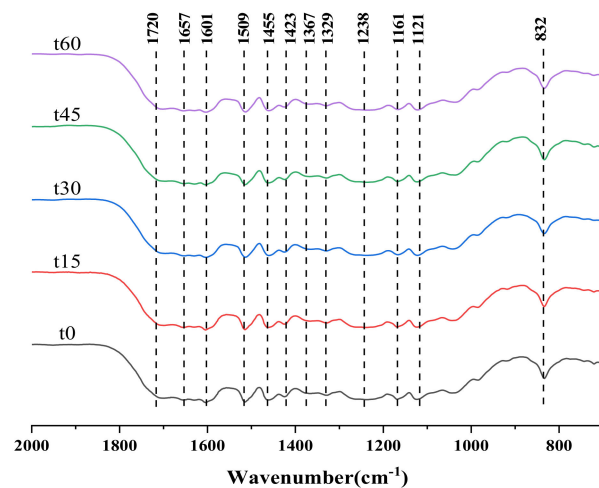


Figure 7. Infrared spectra of lignin obtained by the different sonication time treatments.

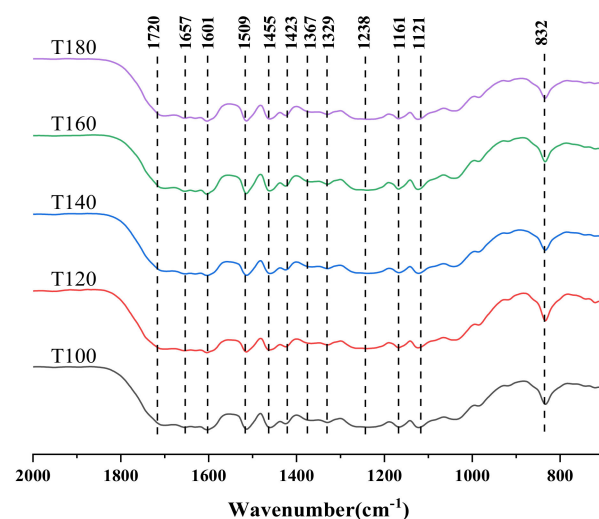


Figure 8. Infrared spectra of lignin obtained by different ultrasonic temperature treatments.

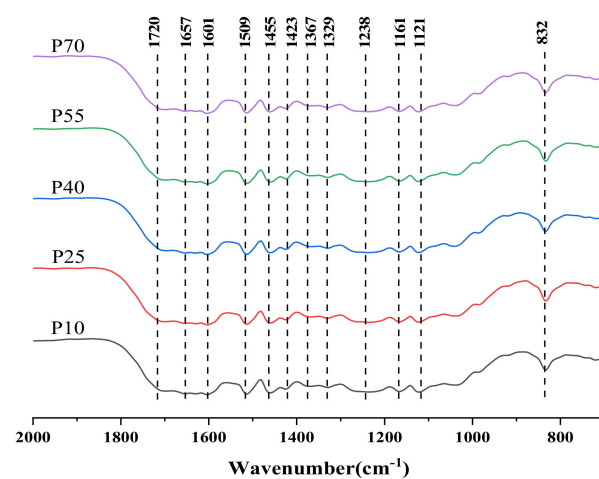


Figure 9. Infrared spectra of lignin obtained by different ultrasonic power treatments.

### 3.6. Hydrothermal–Ultrasonic Ethanol Method for Mass Flow Analysis

In order to investigate the role of ultrasound in the hydrothermal–ethanol method, the mass flow of the three major components of hydrothermal straw was analyzed. Figure 10a shows the hydrothermal–ethanol method, with the experimental conditions of 180 °C and 30 min, and Figure 10b shows the hydrothermal–ultrasonic ethanol method with the experimental conditions of 180 °C, 40%, and 30 min. Figure 10a,b have the same temperature and time; the only difference is the influence of ultrasound. It can be seen in the Figures that the retention of cellulose, and the removal of lignin can be favorably increased in the solid product obtained with the effect of ultrasound. When compared with the hydrothermal–ethanol method, the cellulose content of 51.03% was much greater than that of 42.27% in the hydrothermal–ultrasonic ethanol method, and the lignin content of 12.58% was lower than that of 14.84% in the hydrothermal–ethanol method.

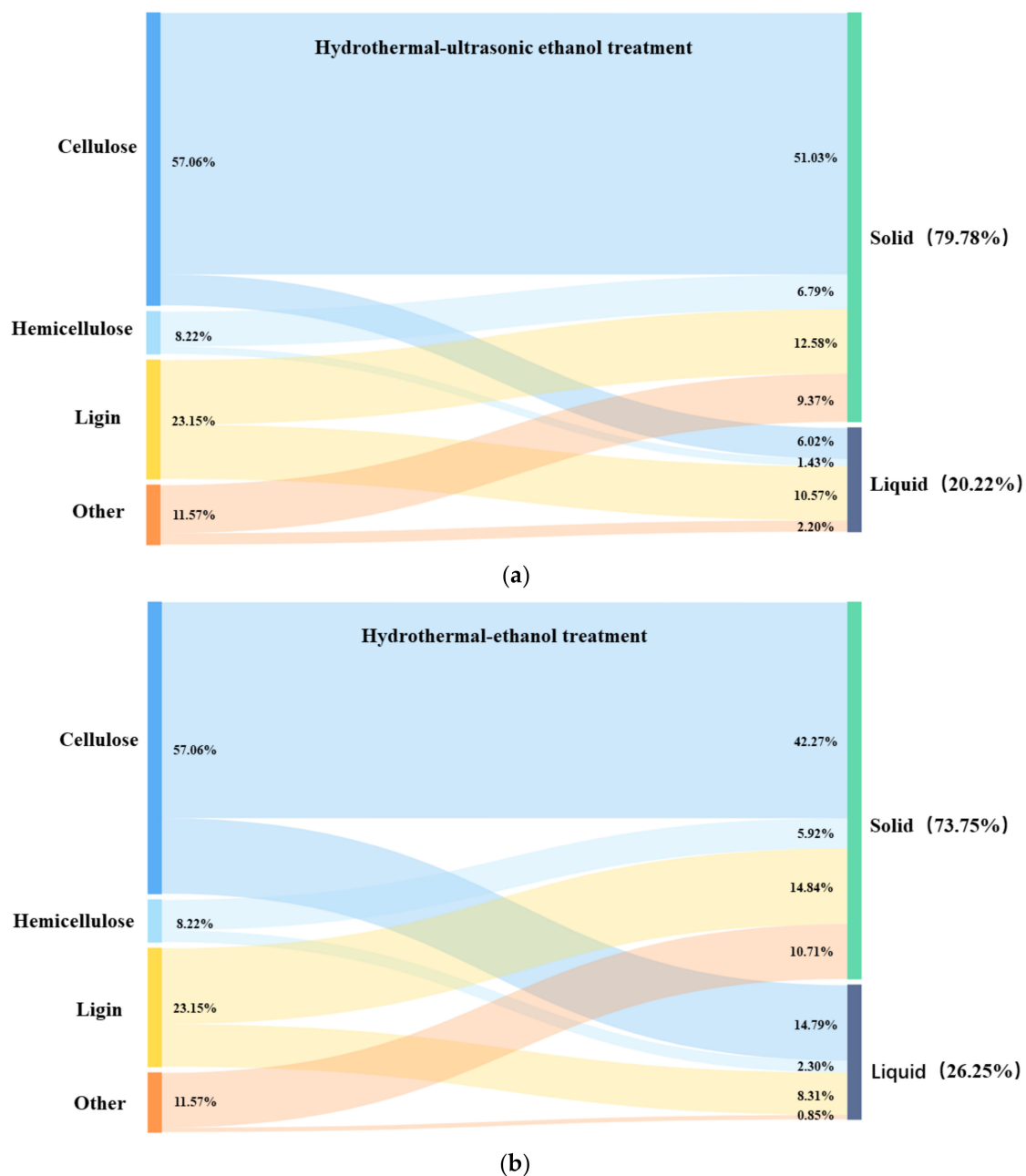


Figure 10. Diagram of the three-component mass flow of hydrothermal straw.

In the process of ultrasound-assisted hydrothermal–ethanol treatment, most of the cellulose was retained and existed in the solid, and only a small portion of small vimentin was hydrolyzed and converted into monosaccharides and furfuryl alcohol, and then hydrolyzed to obtain ethyl formate under the catalytic effect of  $H^+$ . A part of hemicellulose was also present in the solid, which was mainly stabilized by hydrogen bonding with cellulose, leading to difficulty in detachment; thus, it remained in the solid product. A portion of lignin fused to ethanol to produce ethanolic lignin, and a portion of lignin continued to participate in the solid product, which required higher processing conditions for the purpose of removal. Ultrasonic ethanol treatment can better retain the cellulose fraction and remove the lignin fraction.

#### 4. Conclusions

In this study, ultrasound was found to enhance the efficiency of the hydrothermal–ethanol method for the separation of lignocellulosic biomass fractions. The hydrothermal–ultrasonic ethanol method can effectively improve cellulose retention and lignin removal, and the analysis of the obtained organic lignin revealed that there was little effect on the lignin structure. The effects of ultrasonic time, ultrasonic temperature, and ultrasonic power on lignin were also investigated, and a comprehensive analysis of the factors yielded the optimal process as follows: the optimal sonication time was 15 min, the optimal sonication temperature was 180 °C, and the sonication power was 70% (840 W). A longer sonication time will be accompanied by the aggregation of lignin and affect the lignin removal rate. A higher sonication temperature will reduce the retention of cellulose. However, a high sonication power is beneficial for cellulose retention and lignin removal.

**Author Contributions:** Conceptualization: C.T., analysis and investigation: N.Z.; writing and preparation of manuscript: N.Z., C.T.; funding acquisition: C.T., Q.Y., P.F., Y.Z., Z.L. and W.Y. All authors have read and agreed to the published version of the manuscript.

**Funding:** This research was supported by the National Natural Science Foundation of China (51706126, and 31872400), National key research and development program of China (2019YFD1100600), Shandong University of Technology and Zibo City Integration Development Project (2019ZBXC380), and the Youth Innovation Support Program of Shandong Colleges and Universities (2019KJD013).

**Institutional Review Board Statement:** Not applicable.

**Informed Consent Statement:** Not applicable.

**Data Availability Statement:** No new data were created or analyzed in this study. Data sharing is not applicable to this article.

**Acknowledgments:** We gratefully thank to the Analysis and Testing Center in Shandong University of Technology for XRD and FT-IR analyses and Haifeng Zhao.

**Conflicts of Interest:** The authors declare no conflict of interest.

#### References

1. Bhatia, S.K.; Jagtap, S.S.; Bedekar, A.A.; Bhatia, R.K.; Patel, A.K.; Pant, D.; Rajesh Banu, J.; Rao, C.V.; Kim, Y.; Yang, Y. Recent developments in pretreatment technologies on lignocellulosic biomass: Effect of key parameters, technological improvements, and challenges. *Bioresour. Technol.* **2020**, *300*, 122724. [[CrossRef](#)] [[PubMed](#)]
2. Haldar, D.; Purkait, M.K. A review on the environment-friendly emerging techniques for pretreatment of lignocellulosic biomass: Mechanistic insight and advancements. *Chemosphere* **2021**, *264*, 128523. [[CrossRef](#)] [[PubMed](#)]
3. Kumar, B.; Bhardwaj, N.; Agrawal, K.; Chaturvedi, V.; Verma, P. Current perspective on pretreatment technologies using lignocellulosic biomass: An emerging biorefinery concept. *Fuel Process. Technol.* **2020**, *199*, 106244. [[CrossRef](#)]
4. Soltanian, S.; Aghbashlo, M.; Almasi, F.; Hosseinzadeh-Bandbafha, H.; Nizami, A.; Ok, Y.S.; Lam, S.S.; Tabatabaei, M. A critical review of the effects of pretreatment methods on the exergetic aspects of lignocellulosic biofuels. *Energy Convers. Manag.* **2020**, *212*, 112792. [[CrossRef](#)]
5. Vu, H.P.; Nguyen, L.N.; Vu, M.T.; Johir MA, H.; Mclaughlan, R.; Nghiem, L.D. A comprehensive review on the framework to valorise lignocellulosic biomass as biorefinery feedstocks. *Sci. Total Environ.* **2020**, *743*, 140630. [[CrossRef](#)] [[PubMed](#)]

6. Alonso, D.M.; Hakim, S.H.; Zhou, S.; Won, W.; Hosseinaei, O.; Tao, J.; Garcia-Negron, V.; Motagamwala, A.H.; Mellmer, M.A.; Huang, K.; et al. Increasing the revenue from lignocellulosic biomass: Maximizing feedstock utilization. *Sci. Adv.* **2017**, *3*, 1603301. [\[CrossRef\]](#)
7. Sankaran, R.; Parra Cruz, R.A.; Pakalapati, H.; Show, P.L.; Ling, T.C.; Chen, W.; Tao, Y. Recent advances in the pretreatment of microalgal and lignocellulosic biomass: A comprehensive review. *Bioresour. Technol.* **2020**, *298*, 122476. [\[CrossRef\]](#)
8. Sheng, Y.; Lam, S.S.; Wu, Y.; Ge, S.; Wu, J.; Cai, L.; Huang, Z.; Le, Q.V.; Sonne, C.; Xia, C. Enzymatic conversion of pretreated lignocellulosic biomass: A review on influence of structural changes of lignin. *Bioresour. Technol.* **2021**, *324*, 124631. [\[CrossRef\]](#)
9. Hoang, A.T.; Nizetic, S.; Ong, H.C.; Chong, C.T.; Atabani, A.E.; Pham, V.V. Acid-based lignocellulosic biomass biorefinery for bioenergy production: Advantages, application constraints, and perspectives. *J. Environ. Manag.* **2021**, *296*, 113194. [\[CrossRef\]](#)
10. Ab Rasid, N.S.; Shamjuddin, A.; Abdul Rahman, A.Z.; Amin NA, S. Recent advances in green pre-treatment methods of lignocellulosic biomass for enhanced biofuel production. *J. Clean. Prod.* **2021**, *321*, 129038. [\[CrossRef\]](#)
11. Haldar, D.; Purkait, M.K. Lignocellulosic conversion into value-added products: A review. *Process Biochem.* **2020**, *89*, 110–133. [\[CrossRef\]](#)
12. Meng, X.; Bhagia, S.; Wang, Y.; Zhou, Y.; Pu, Y.; Dunlap, J.R.; Shuai, L.; Ragauskas, A.J.; Yoo, C.G. Effects of the advanced organosolv pretreatment strategies on structural properties of woody biomass. *Ind. Crops Prod.* **2020**, *146*, 112144. [\[CrossRef\]](#)
13. Ong, V.Z.; Wu, T.Y. An application of ultrasonication in lignocellulosic biomass valorisation into bio-energy and bio-based products. *Renew. Sustain. Energy Rev.* **2020**, *132*, 109924. [\[CrossRef\]](#)
14. Huerta, R.R.; Silva, E.K.; Ekaette, I.; El-Bialy, T.; Saldaña MD, A. High-intensity ultrasound-assisted formation of cellulose nanofiber scaffold with low and high lignin content and their cytocompatibility with gingival fibroblast cells. *Ultrason. Sonochem.* **2020**, *64*, 104759. [\[CrossRef\]](#)
15. Bundhoo, Z.M.A.; Mohee, R. Ultrasound-assisted biological conversion of biomass and waste materials to biofuels: A review. *Ultrason. Sonochem.* **2018**, *40*, 298–313. [\[CrossRef\]](#)
16. Li, J.; Feng, P.; Xiu, H.; Zhang, M.; Li, J.; Du, M.; Zhang, X.; Kozliak, E.; Ji, Y. Wheat straw components fractionation, with efficient delignification, by hydrothermal treatment followed by facilitated ethanol extraction. *Bioresour. Technol.* **2020**, *316*, 123882. [\[CrossRef\]](#)
17. Li, J.; Feng, P.; Xiu, H.; Li, J.; Yang, X.; Ma, F.; Li, X.; Zhang, X.; Kozliak, E.; Ji, Y. Morphological changes of lignin during separation of wheat straw components by the hydrothermal-ethanol method. *Bioresour. Technol.* **2019**, *294*, 122157. [\[CrossRef\]](#)
18. Choi, J.; Park, S.; Kim, J.; Cho, S.; Jang, S.; Hong, C.; Choi, I. Selective deconstruction of hemicellulose and lignin with producing derivatives by sequential pretreatment process for biorefining concept. *Bioresour. Technol.* **2019**, *291*, 121913. [\[CrossRef\]](#)
19. Yin, S.; Zhang, N.; Tian, C.; Yi, W.; Yuan, Q.; Fu, P.; Zhang, Y.; Li, Z. Effect of Accumulative Recycling of Aqueous Phase on the Properties of Hydrothermal Degradation of Dry Biomass and Bio-Crude Oil Formation. *Energies* **2021**, *14*, 285. [\[CrossRef\]](#)
20. Guo, X.; Liu, S.; Wang, Z.; Zhang, G. Ultrasonic-assisted extraction of polysaccharide from *Dendrobium officinale*: Kinetics, thermodynamics and optimization. *Biochem. Eng. J.* **2022**, *177*, 108227. [\[CrossRef\]](#)
21. Akhlisah, Z.N.; Yunus, R.; Abidin, Z.Z.; Lim, B.Y.; Kania, D. Pretreatment methods for an effective conversion of oil palm biomass into sugars and high-value chemicals. *Biomass Bioenergy* **2021**, *144*, 105901. [\[CrossRef\]](#)
22. Xu, J.; Zhang, S.; Shi, Y.; Zhang, P.; Huang, D.; Lin, C.; Wu, Y. Upgrading the wood vinegar prepared from the pyrolysis of biomass wastes by hydrothermal pretreatment. *Energy* **2021**, *244*, 122631. [\[CrossRef\]](#)
23. Silva, A.C.; Barbosa, M.S.; Barral, U.M.; Silva BP, C.; Fernandes JS, C.; Viana AJ, S.; Filho CV, M.; Bispo DF, A.; Christófar, C.; Ragonezi, C.; et al. Organic matter composition and paleoclimatic changes in tropical mountain peatlands currently under grasslands and forest clusters. *CATENA* **2019**, *180*, 69–82. [\[CrossRef\]](#)
24. Xu, Q.; Zhao, M.; Yu, Z.; Yin, J.; Li, G.; Zhen, M.; Zhang, Q. Enhancing enzymatic hydrolysis of corn cob, corn stalk and sorghum stalk by dilute aqueous ammonia combined with ultrasonic pretreatment. *Ind. Crops Prod.* **2017**, *109*, 220–226. [\[CrossRef\]](#)
25. Manzato, L.; Rabelo LC, A.; De Souza, S.M.; Da Silva, C.G.; Sanches, E.A.; Rabelo, D.; Mariuba LA, M.; Simonsen, J. New approach for extraction of cellulose from tucumã's endocarp and its structural characterization. *J. Mol. Struct.* **2017**, *1143*, 229–234. [\[CrossRef\]](#)
26. Rizwan, M.; Gilani, S.R.; Durrani, A.I.; Naseem, S. Cellulose extraction of *Alstonia scholaris*: A comparative study on efficiency of different bleaching reagents for its isolation and characterization. *Int. J. Biol. Macromol.* **2021**, *191*, 964–972. [\[CrossRef\]](#)
27. Chen, X.; Li, H.; Sun, S.; Cao, X.; Sun, R. Co-production of oligosaccharides and fermentable sugar from wheat straw by hydrothermal pretreatment combined with alkaline ethanol extraction. *Ind. Crops Prod.* **2018**, *111*, 78–85. [\[CrossRef\]](#)
28. Rao, M.V.; Sengar, A.S.; CK, S.; Rawson, A. Ultrasonication—A green technology extraction technique for spices: A review. *Trends Food Sci. Technol.* **2021**, *116*, 975–991. [\[CrossRef\]](#)
29. Muthuvelu, K.S.; Rajarathinam, R.; Kanagaraj, L.P.; Ranganathan, R.V.; Dhanasekaran, K.; Manickam, N.K. Evaluation and characterization of novel sources of sustainable lignocellulosic residues for bioethanol production using ultrasound-assisted alkaline pre-treatment. *Waste Manag.* **2019**, *87*, 368–374. [\[CrossRef\]](#) [\[PubMed\]](#)
30. Luo, J.; Fang, Z.; Smith, R.L. Ultrasound-enhanced conversion of biomass to biofuels. *Prog. Energy Combust. Sci.* **2014**, *41*, 56–93. [\[CrossRef\]](#)
31. Louis AC, F.; Venkatachalam, S. Energy efficient process for valorization of corn cob as a source for nanocrystalline cellulose and hemicellulose production. *Int. J. Biol. Macromol.* **2020**, *163*, 260–269. [\[CrossRef\]](#)



32. Koutsianitis, D.; Mitani, C.; Giagli, K.; Tsalagkas, D.; Halász, K.; Kolonics, O.; Gallis, C.; Csóka, L. Properties of ultrasound extracted bicomponent lignocellulose thin films. *Ultrason. Sonochem.* **2015**, *23*, 148–155. [\[CrossRef\]](#)
33. Wang, Q.; Niu, L.; Jiao, J.; Guo, N.; Zang, Y.; Gai, Q.; Fu, Y. Degradation of lignin in birch sawdust treated by a novel *Myrothecium verrucaria* coupled with ultrasound assistance. *Bioresour. Technol.* **2017**, *244*, 969–974. [\[CrossRef\]](#)
34. Wang, S.; Li, F.; Zhang, P.; Jin, S.; Tao, X.; Tang, X.; Ye, J.; Nabi, M.; Wang, H. Ultrasound assisted alkaline pretreatment to enhance enzymatic saccharification of grass clipping. *Energy Convers. Manag.* **2017**, *149*, 409–415. [\[CrossRef\]](#)
35. Singh, S.; Agarwal, M.; Bhatt, A.; Goyal, A.; Moholkar, V.S. Ultrasound enhanced enzymatic hydrolysis of *Parthenium hysterophorus*: A mechanistic investigation. *Bioresour. Technol.* **2015**, *192*, 636–645. [\[CrossRef\]](#)
36. Bussemaker, M.J.; Xu, F.; Zhang, D. Manipulation of ultrasonic effects on lignocellulose by varying the frequency, particle size, loading and stirring. *Bioresour. Technol.* **2013**, *148*, 15–23. [\[CrossRef\]](#)
37. Zhou, Z.; Liu, D.; Zhao, X. Conversion of lignocellulose to biofuels and chemicals via sugar platform: An updated review on chemistry and mechanisms of acid hydrolysis of lignocellulose. *Renew. Sustain. Energy Rev.* **2021**, *146*, 111169. [\[CrossRef\]](#)
38. Zhou, M.; Tian, X. Development of different pretreatments and related technologies for efficient biomass conversion of lignocellulose. *Int. J. Biol. Macromol.* **2022**, *10*, 2741. [\[CrossRef\]](#)
39. Xu, Y.; Li, M. Hydrothermal liquefaction of lignocellulose for value-added products: Mechanism, parameter and production application. *Bioresour. Technol.* **2021**, *342*, 126035. [\[CrossRef\]](#)
40. Sun, Q.; Chen, W.; Pang, B.; Sun, Z.; Lam, S.S.; Sonne, C.; Yuan, T. Ultrastructural change in lignocellulosic biomass during hydrothermal pretreatment. *Bioresour. Technol.* **2021**, *341*, 125807. [\[CrossRef\]](#)
41. Sarker, T.R.; Pattnaik, F.; Nanda, S.; Dalai, A.K.; Meda, V.; Naik, S. Hydrothermal pretreatment technologies for lignocellulosic biomass: A review of steam explosion and subcritical water hydrolysis. *Chemosphere* **2021**, *284*, 131372. [\[CrossRef\]](#)
42. Shchukin, D.G.; Skorb, E.; Belova, V.; Möhwald, H. Ultrasonic Cavitation at Solid Surfaces. *Adv. Mater.* **2011**, *23*, 1922–1934. [\[CrossRef\]](#)
43. García, A.; Erdocia, X.; González Alriols, M.; Labidi, J. Effect of ultrasound treatment on the physicochemical properties of alkaline lignin. *Chem. Eng. Process. Process Intensif.* **2012**, *62*, 150–158. [\[CrossRef\]](#)
44. Sun, R.; Tomkinson, J. Comparative study of lignins isolated by alkali and ultrasound-assisted alkali extractions from wheat straw. *Ultrason. Sonochem.* **2002**, *9*, 85–93. [\[CrossRef\]](#)
45. García, A.; Alriols, M.G.; Llano-Ponte, R.; Labidi, J. Ultrasound-assisted fractionation of the lignocellulosic material. *Bioresour. Technol.* **2011**, *102*, 6326–6330. [\[CrossRef\]](#)
46. Liu, X.; Jiang, Z.; Feng, S.; Zhang, H.; Li, J.; Hu, C. Catalytic depolymerization of organosolv lignin to phenolic monomers and low molecular weight oligomers. *Fuel* **2019**, *244*, 247–257. [\[CrossRef\]](#)
47. Wang, K.; Wang, B.; Hu, R.; Zhao, X.; Li, H.; Zhou, G.; Song, L.; Wu, A. Characterization of hemicelluloses in *Phyllostachys edulis* (moso bamboo) culm during xylogenesis. *Carbohydr. Polym.* **2019**, *221*, 127–136. [\[CrossRef\]](#)
48. Choi, J.; Jang, S.; Kim, J.; Park, S.; Kim, J.; Jeong, H.; Kim, H.; Choi, I. Simultaneous production of glucose, furfural, and ethanol organosolv lignin for total utilization of high recalcitrant biomass by organosolv pretreatment. *Renew. Energy* **2019**, *130*, 952–960. [\[CrossRef\]](#)
49. Kawamata, Y.; Yoshikawa, T.; Aoki, H.; Koyama, Y.; Nakasaka, Y.; Yoshida, M.; Masuda, T. Kinetic analysis of delignification of cedar wood during organosolv treatment with a two-phase solvent using the unreacted-core model. *Chem. Eng. J.* **2019**, *368*, 71–78. [\[CrossRef\]](#)
50. Utekar, P.G.; Kininge, M.M.; Gogate, P.R. Intensification of delignification and enzymatic hydrolysis of orange peel waste using ultrasound for enhanced fermentable sugar production. *Chem. Eng. Process. Process Intensif.* **2021**, *168*, 108556. [\[CrossRef\]](#)
51. Wu, H.; Dai, X.; Zhou, S.L.; Gan, Y.Y.; Xiong, Z.Y.; Qin, Y.H.; Ma, J.; Yang, L.; Wu, Z.K.; Wang, T.L. Ultrasound-assisted alkaline pretreatment for enhancing the enzymatic hydrolysis of rice straw by using the heat energy dissipated from ultrasonication. *Bioresour. Technol.* **2017**, *241*, 70–74. [\[CrossRef\]](#) [\[PubMed\]](#)
52. Mongkolpichayarak, I.; Jiraroj, D.; Anutrasakda, W.; Ngamcharussrivichai, C.; Samec JS, M.; Tungasmita, D.N. Cr/MCM-22 catalyst for the synthesis of levulinic acid from green hydrothermolysis of renewable biomass resources. *J. Catal.* **2022**, *405*, 373–384. [\[CrossRef\]](#)
53. Fang, W.; Riisager, A. Efficient valorization of biomass-derived furfural to fuel bio-additive over aluminum phosphate. *Appl. Catal. B Environ.* **2021**, *298*, 120575. [\[CrossRef\]](#)
54. El Hage, R.; Brosse, N.; Chrusciel, L.; Sanchez, C.; Sannigrahi, P.; Ragauskas, A. Characterization of milled wood lignin and ethanol organosolv lignin from miscanthus. *Polym. Degrad. Stab.* **2009**, *94*, 1632–1638. [\[CrossRef\]](#)
55. Liu, L.; Patankar, S.C.; Chandra, R.P.; Sathitsuksanoh, N.; Saddler, J.N.; Renneckar, S. Valorization of Bark Using Ethanol–Water Organosolv Treatment: Isolation and Characterization of Crude Lignin. *ACS Sustain. Chem. Eng.* **2020**, *8*, 4745–4754. [\[CrossRef\]](#)
56. Cheng, X.; Guo, X.; Qin, Z.; Wang, X.; Liu, H.; Liu, Y. Structural features and antioxidant activities of Chinese quince (*Chaenomeles sinensis*) fruits lignin during auto-catalyzed ethanol organosolv pretreatment. *Int. J. Biol. Macromol.* **2020**, *164*, 4348–4358. [\[CrossRef\]](#) [\[PubMed\]](#)
57. Zevallos Torres, L.A.; Lorenci Woiciechowski, A.; De Andrade Tanobe, V.O.; Karp, S.G.; Guimarães Lorenci, L.C.; Faulds, C.; Soccol, C.R. Lignin as a potential source of high-added value compounds: A review. *J. Clean. Prod.* **2020**, *263*, 121499. [\[CrossRef\]](#)
58. Sheng, Y.; Ma, Z.; Wang, X.; Han, Y. Ethanol organosolv lignin from different agricultural residues: Toward basic structural units and antioxidant activity. *Food Chem.* **2022**, *376*, 131895. [\[CrossRef\]](#)